Chance-constrained Calculation of the Reserve Service Provided by EV Charging Station Clusters in Energy Communities

Published Version:
Chance-constrained Calculation of the Reserve Service Provided by EV Charging Station Clusters in Energy Communities / Marasciuolo F.; Orozco C.; Dicorato M.; Borghetti A.; Forte G.. - In: IEEE TRANSACTIONS ON INDUSTRY APPLICATIONS. - ISSN 0093-9994. - STAMPA. - 59:4(2023), pp. 10094006.1-10094006.10. [10.1109/TIA.2023.3264965]

Availability:
This version is available at: https://hdl.handle.net/11585/928679 since: 2023-11-24

Published:
DOI: http://doi.org/10.1109/TIA.2023.3264965

Marasciuolo, F., Orozco, C., Dicorato, M., Borghetti, A., & Forte, G. (2023). Chance-constrained Calculation of the Reserve Service Provided by EV Charging Station Clusters in Energy Communities. *IEEE Transactions on Industry Applications*. https://doi.org/10.1109/TIA.2023.3264965

Chance-constrained Calculation of the Reserve Service Provided by EV Charging Station Clusters in Energy Communities

F. Marasciuolo, *Student Member, IEEE,* C. Orozco, *Student Member, IEEE,* M. Dicorato, *Member, IEEE,* A. Borghetti, *Member, IEEE,* and G. Forte, *Member, IEEE*

***Abstract*— The concept of energy community is currently under investigation as it is considered central into the energy transition process. One of the main aspects of the successful implementation of community lays in the energy management system that coordinates exchanges among prosumers. This paper deals with the optimal energy management of a local energy community of dc microgrids with electric vehicle charging stations, considering local reserve provided by storage units and vehicle batteries. A two-stage optimal procedure is proposed to assess the optimal scheduling of resources for each community participant. Additionally, the optimal up and down reserve levels able to cover random fluctuations in photovoltaic generation within each EV-based microgrid are determined by a set of specific chance constraints.**

***Index Terms*— energy community, DC microgrid, electric vehicles, vehicle-to-grid, operation cost, grid power exchange, reserve provision**

NOMENCLATURE

A. First stage energy community scheduling

1) Objective function terms

$C_{\mathrm{b\_G}\,i}(t)$	cost for purchased energy by *i*-th prosumer from the utility grid at *t*-th time-step
$C_{\mathrm{b}\,i,j}(t)$	cost for purchased energy by *i*-th prosumer from other *j*-th prosumers of the community at *t*-th time-step
$S_{\mathrm{s\_G}\,i}(t)$	revenue for selling energy by *i*-th prosumer to the utility grid at *t*-th time-step
$S_{\mathrm{s}\,i,j}(t)$	revenue for selling energy by *i*-th prosumer to other *j*-th prosumers of the community at *t*-th time-step
$\ell_i(t)$	penalty function of the square imbalances of the power exchanges of *i*-th prosumer at *t*-th time-step
$C_S(t)$	costs for the use of charging stations *i*-th prosumer at *t*-th time-step
$W_{\mathrm{BES}}(t)$	costs for the use of battery energy storage (BES) units at *t*-th time-step

2) Parameters

$\pi_{\mathrm{buy}}(t)$	tariff applied to *i*-th prosumer buying energy from the utility grid at *t*-th time-step
$\pi_{\mathrm{sell}}(t)$	tariff applied to *i*-th prosumer selling energy to the utility grid at *t*-th time-step
Δt	duration of each time-step
t	index for time-step
i , j	index for prosumer
n_t	total number of time-steps in the time horizon
w_{BES}	average wearing cost associated with charging and discharging of BES units
w_{EV}	average wearing cost associated with charging and discharging of the EV batteries

3) Variables

$P_{\mathrm{b\_G}\,i}(t)$	power bought by *i*-th prosumer from with the utility grid at *t*-th time-step
$P_{\mathrm{s\_G}\,i}(t)$	power sold by *i*-th prosumer to with the utility grid at *t*-th time-step
$P_{\mathrm{b}\,i,j}(t)$	power bought by *i*-th prosumer from the *j*-th prosumer at *t*-th time-step
$P_{\mathrm{s}\,i,j}(t)$	power sold by *i*-th prosumer to the *j*-th prosumer at *t*-th time-step
$\lambda_i(t)$	Lagrangian multiplier associated to the equilibrium of power exchange of the *i*-th prosumer at *t*-th time-step
$P_{\mathrm{BES\,ch}\,i}(t)$	charging power of the BES unit of the *i*-th prosumer at *t*-th time-step
$P_{\mathrm{BES\,dis}\,i}(t)$	discharging power of the BES unit of the *i*-th prosumer at *t*-th time-step
$P_{\mathrm{Clust\,EV,i}}(t)$	power output of EV station cluster of the *i*-th prosumer at *t*-th time-step

B. Second stage DC microgrid programming

1) Objective function terms

$D_{in}^2(t)$	quadratic deviation of bought power by the microgrid in *t*-th time-step w.r.t. first level yields
$D_{out}^2(t)$	quadratic deviation of sold power by the microgrid in *t*-th time-step w.r.t. first level yields

This document has been created in the context of the PROGRESSUS project. The PROGRESSUS project has received funding from the Electronic Components and Systems for European Leadership Joint Undertaking under grant agreement No 876868. This Joint Undertaking receives support from the European Union's Horizon 2020 research and innovation programme and Germany, Slovakia, Netherlands, Spain, Italy.

F. Marasciuolo, M. Dicorato and G. Forte are with the Dept. of Electrical and Information Engineering, Politecnico di Bari, Bari, Italy (corresponding: F. Marasciuolo, e-mail: francesca.marasciuolo@poliba.it)

A. Borghetti and C. Orozco are with the Dept. of Electrical, Electronic and Information Engineering, University of Bologna, Bologna, Italy.

$OC_{MG}(t)$ operating cost of the microgrid in t-th time-step
ρ weighting factor

2) Parameters

w_b wearing cost associated to *b*-th BES
w_k wearing cost associated to *k*-th EV
$c_{ev}(t)$ charging costs for EV at *t*-th time-step
$r_{ev}(t)$ revenue for EV discharge at *t*-th time-step
k index for electric vehicles (EV)
b index for BESs
n_{ev} total number of EVs in the microgrid
$P_{PV}(t)$ forecast power generation by photovoltaic (PV) system at *t*-th time step
η_g coefficient for converter efficiency and cable losses on connection grid-DC busbar
η_b coefficient for converter efficiency and cable losses on connection BES-DC busbar
$\eta_{ev,k}$ coefficient for converter efficiency and cable losses on connection EV-DC busbar
η_{PV} coefficient for converter efficiency and cable losses on connection PV system-DC busbar
γ_b^c charge efficiency of *b*-th BES
γ_b^d discharge efficiency of *b*-th BES
sd_b self-discharge rate of *b*-th BES
$\gamma_{ev,k}^c$ charge efficiency of *k*-th EV
$\gamma_{ev,k}^d$ discharge efficiency of *k*-th EV
$sd_{ev,k}$ self-discharge rate of *k*-th EV
$\Delta E_{ev,k}^{trip}(t)$ energy amount necessary for envisaged trips of the *k*-th EV in the *t*-th time-step
$P_{g,MAX}^{in}$ maximum level of power withdrawal by the microgrid from the grid
$P_{g,MAX}^{out}$ maximum level of power delivery by the microgrid to the grid
$SOC_b^{\min}$ minimum state-of-charge (SOC) of the *b*-th BES
$SOC_b^{\max}$ maximum SOC level of the *b*-th BES
$P_b^{d,nom}$ maximum discharge power of the *b*-th BES
$P_b^{c,nom}$ maximum charge power of the *b*-th BES
$SOC_{ev,k}^{\min}$ minimum SOC level of the *k*-th EV
$SOC_{ev,k}^{\max}$ maximum SOC level of the *k*-th EV
$P_{ev,k}^{d,nom}$ maximum discharge power of the *k*-th EV
$P_{ev,k}^{c,nom}$ maximum charge power of the k-th EV

3) Variables

$P_g^{in}(t)$ power withdrawal by the microgrid from the grid at *t*-th time-step
$P_g^{in}(t)$ power delivery by the microgrid from the grid at *t*-th time-step
$P_b^c(t)$ charge power of the *b*-th BES at *t*-th time step
$P_b^d(t)$ discharge power of the *b*-th BES at *t*-th time step
$P_{ev,k}^c(t)$ charge power of the *k*-th EV at *t*-th time step
$P_{ev,k}^d(t)$ discharge power of the *k*-th EV at *t*-th time step
$SOC_b(t)$ SOC level of the *b*-th BES at *t*-th time step
$SOC_{ev,k}(t)$ SOC level of the *k*-th EV at *t*-th time step
$\upsilon_g(t)$ binary variable for power exchange direction at grid connection at *t*-th time step
$\upsilon_b(t)$ binary variable for power exchange direction by *b*-th BES at *t*-th time step
$\upsilon_{ev,k}(t)$ binary variable for power exchange direction by *k*-th EV at *t*-th time step

C. Stochastic approach

1) Additional Parameters

$P_{PV}^{act}(t)$ actual power production by PV system at *t*-th time step
$\varepsilon_{PV}(t)$ forecasting error of power production by PV system at *t*-th time step
$\varepsilon(t)$ net forecasting error at *t*-th time-step
$\alpha^+(t)$ accepted probability of positive reserve constraint violation at *t*-th time-step
$\alpha^-(t)$ accepted probability of negative reserve constraint violation at *t*-th time-step
$q_{1-\alpha^+}^+(t)$ $(1-\alpha^+)$ -th quantile of net forecasting error distribution at *t*-th time-step
$q_{1-\alpha^-}^-(t)$ $(1-\alpha^-)$ -th quantile of net forecasting error distribution at *t*-th time-step
$\mu_\varepsilon(t)$ mean value of net forecasting error at *t*-th time-step
$\sigma_\varepsilon(t)$ standard deviation of net forecasting error at *t*-th time-step

2) Additional Variables

$R_b^+(t)$ positive reserve by *b*-th BES at *t*-th time-step
$R_b^-(t)$ negative reserve by *b*-th BES at *t*-th time-step
$R_{ev,k}^+(t)$ positive reserve by *k*-th EV at *t*-th time-step
$R_{ev,k}^-(t)$ negative reserve by *k*-th EV at *t*-th time-step

II. Introduction

The energy community concept is now implemented in the regulatory framework of many countries [1]. An energy community enables end users, as prosumers, to share their resources and exchange energy with each other. In this context, the optimal scheduling of the community energy resources by a specifically developed energy management system (EMS) is important. Distributed approaches may be preferred with respect to centralized ones, as they have less communication requirements and better guarantee prosumers' independence [2] [3].

The microgrid structure allows prosumers to coordinate their internal resources, as photovoltaic (PV) and battery energy storage (BES) units, to match local load demand and to reach reliability and economic goals. Moreover, grid-connected microgrids can support the external grid by providing ancillary services, such as frequency control, voltage control and load curtailment operation [4] [5]. In the procedures presented in the literature, multi-microgrid energy management strategies are often based on hierarchical and distributed approaches [6][7], which usually consists of multiple optimization stages. Bi-level optimal procedures are proposed in e.g. [8] for systems of microgrids integrated in the distribution network (DN): in one level, daily costs [9] or profits of DN company [10] are optimized, while the second level optimizes the microgrid costs. A data-driven multi-agent deep reinforcement learning approach is investigated in [11] to calculate the Stackelberg equilibrium for the bi-level optimization problem.

The integration of electric vehicle (EV) charging stations in dc microgrids [12] can be addressed by, e.g., hierarchical distributed procedures, where they are modeled as independent players [13], or by multi-agent deep reinforcement learning methods [14] with the aim of minimizing total costs. The presence of BES and PV units in the microgrids leads to a better performance in terms of cost reduction [15], particularly when vehicle-to-grid services (V2G) are exploited [16] [17].

This paper focuses on the optimal energy management of a local energy community (LEC) of dc microgrids with EV charging stations, in addition to PV and BES units, which represents a promising solution for EV integration [18].

The integration of intermittent energy resources in microgrids [19], as wind and PV generation, as well as the integration of EVs [20], implies to address the management of the associated uncertainties. Therefore, in optimal scheduling procedures, deterministic programming approaches, based on the assumption of perfect forecasts, are replaced by stochastic programming techniques [21]. Monte Carlo and stochastic scenario models are used in [22] to simulate RES generation, load and prices variations, and in [23] to account for driving behavior of EVs. Chance-constrained programming techniques, that imply a mathematical program model containing chance constraints to be satisfied with a suitable probability level, are used to account for uncertainties in renewable generation in a community integrated system, as in [24], and levels of energy outputs of a hybrid ac-dc microgrid [25]. Recurse optimization is adopted in [26] for a day-ahead multistage stochastic scheduling of a LEC that provides a multi-stage decision tree to a receding horizon intra-day optimization procedure. In [27] a scenario tree generation and fast forward scenario reduction is adopted to account for RES generation uncertainties in a 15-bus microgrid test system. Moreover, robust optimization is proposed in [28] for the optimal charging and frequency reserve scheduling of EVs and in [29] for the microgrid reserve scheduling considering uncertainties associated to load, price, and renewable production. Information gap decision theory (IGDT) is used for the representation of reserve probabilities in [30] and [31] in the presence of fluctuations in RES generation and electricity prices. For large-scale systems, distributionally robust optimization procedures are adopted to represent fluctuations of load demand and renewable generation, as in [32] and [33]. Regarding the type of systems under study, chance-constrained programming is implemented in small and medium systems, as microgrids or communities of microgrids, while robust and distributionally robust optimal programming is implemented in larger networks, such as multiple-area grids. Most of procedures included in this comparative analysis do not significantly consider the role of EVs (as in [27], [30], and [31]) or only their charging processes are involved. Further exploitation of V2G functionalities is not investigated, with the exception of [29].

By extending the deterministic two-stage optimal procedure proposed in [34] for the day-ahead energy management of a LEC of dc microgrids with bidirectional EV charging stations, this paper presents a procedure that calculates the optimal scheduling of the community considering the possibility for BES and EV batteries to provide the reserve needed to cope with the uncertainties due to the fluctuations in solar generation.

The main contributions of the procedure are listed and discussed below:

- Chance-constrained programming technique is implemented to EV-based dc microgrids in a LEC to model storage reserves by means of a set of probabilistic constraints in order to counterbalance the uncertainty associated with PV production within the microgrid. Various papers have adopted this technique, thanks to the linearization of stochastic processes, and in particular [25] highlights the advantages with respect to other methods, dealing with uncertainties of the power exchanges with the external grid. In this paper the application of the chance constrained approach is focused on the internal source of uncertainty. Its integration in the alternating direction method of multipliers (ADMM)-based distributed optimization approach used for the day-ahead scheduling of the community resources ensures, at a given confidence level, the respect of the planned power exchanges among the LEC participants during the intraday operation. The effectiveness of chance-constrained method is assessed through a comparison with Monte-Carlo simulation results.
- The flexibility of EV charging stations and BES to provide both up and down reserve is used to compensate the PV forecast uncertainties. Differently from other papers where the reserve is intended to provide grid auxiliary services with the participation in bulk or local markets, as e.g., [35][36][37], in this paper the reserve improves the feasibility of the day-ahead scheduling of the dc microgrids that participates in the energy community.
- The procedure is conceived to be applied for the operation management of a real installation, where the compliance with the LEC planning stage of each microgrid is deemed to have remarkable impact on the other community participants.

The structure of the paper is the following. Section II describes the methodology, the stochastic model for the representation of the reserve provision, and the specific models adopted for BES units and EV charging stations. Section III describes the case study and Section IV the test results. Section V concludes the paper.

III. Methodology

A. General overview

The developed two-stage approach provides the optimal day-ahead scheduling of the resources of a LEC. In the first stage, an ADMM-based optimization approach, described in detail in [38], defines the scheduling of the resources for the next day. As in [35], the community dealt with in this paper includes also microgrids equipped by clusters of bidirectional EV charging stations, other than prosumers equipped with PV systems, storage units, and local loads.

Each prosumer i iteratively solves a local optimization problem coordinated with those of the other prosumers to reach the resource scheduling for the entire community, considering the direct transactions among prosumers other than the transactions of each prosumer with the external energy provider (here identified with the utility grid for simplicity). The objective function of each local optimization (1) represents the daily cost of the prosumer,

$$\min \sum_{t=1}^{n_t} \begin{bmatrix} C_{\mathrm{b\_G}\,i}(t) - S_{\mathrm{s\_G}\,i}(t) + \sum_{j\neq i} C_{\mathrm{b}\,i,j}(t) \\ -\sum_{j\neq i} S_{\mathrm{s}\,i,j}(t) + C_S(t) + W_{\mathrm{BES}}(t) + \ell_i(t) \end{bmatrix} \qquad (1)$$

being $C_{\mathrm{b\_G}\,i}(t) = \pi_{\mathrm{b}}(t) P_{\mathrm{b\_G}\,i}(t)\Delta t$, $S_{\mathrm{s\_G}\,i}(t) = \pi_{\mathrm{s}}(t) P_{\mathrm{s\_G}\,i}(t)\Delta t$, $C_{\mathrm{b}\,i,j}(t) = \lambda_j(t) P_{\mathrm{b}\,i,j}(t)\Delta t$, $S_{\mathrm{s}\,i,j}(t) = \lambda_i(t) P_{\mathrm{s}\,i,j}(t)\Delta t$, $C_S \geq w_{\mathrm{EV}} P_{\mathrm{Clust\,EV}}(t)\Delta t$ and $C_S(t) \geq -w_{\mathrm{EV}} P_{\mathrm{Clust\,EV}}(t)\Delta t$, $W_{\mathrm{BES}}(t) = w_{\mathrm{BES}}\left(P_{\mathrm{BESch}\,i}(t) + P_{\mathrm{BESdis}\,i}(t)\right)\Delta t$. The penalty function $\ell_i(t)$ and Lagrangian multipliers $\lambda_i(t)$ and $\lambda_j(t)$ are updated at each ADMM iteration. A forecast of the EV trips provides the time of departure and arrival for each EV together with the corresponding decrease in the energy stored in the EV's battery during each trip. Based on this information and the setting of the desired SoC at the departure of each EV, the proposed procedure calculates the total energy entering the microgrid due to arrivals of EVs and the total energy leaving due to EV departures at time t, which are inputs of the optimization model. Local constraints, i.e., the ones described in [38] and in [17] for prosumers and for microgrids with EV charging stations, respectively, complete the model.

The iterative ADMM procedure reaches the convergence when all $\ell_i(t)$ become smaller than a predefined tolerance for each decoupled optimization i relevant to a community participant. At the convergence, the first stage calculates the optimal scheduling of energy transactions with the external energy provider, energy transactions with other participants inside the community, the operation of the own BES unit, and, in the case of microgrids equipped with cluster of EVs' charging stations, the total power outputs of the EV cluster. The price for each energy transaction inside the community is also obtained. The optimal energy transactions among the prosumers within the community and with the external utility grid evaluated by the first stage are provided to the second stage optimization.

For each EV-based microgrid, the second stage optimization defines the individual scheduling of each charging station, keeping the feasibility of the global solution of the energy community. The second stage optimization fully exploits the availability of V2G services provided by the EVs connected to bidirectional charging stations. The state variables to be optimized include the withdrawn and injected powers at the common coupling point (PCC), BES and EV charging/discharging powers and the battery state of charge (SOC) levels. The objective function of the second stage (2) aims at minimizing the sum of quadratic deviations of bought and sold power in each time-step and the operating costs of the microgrid (3), multiplied by a weighted factor ρ (which is set in the study to 10 kWh^2/€. The operating cost function includes EV charging costs, revenues for EV discharging and wearing costs associated to BES and EV exploitations as in [34].

$$\min \sum_t D_{in}^2(t) + D_{out}^2(t) + \rho \cdot OC_{MG}(t) \qquad (2)$$

$$\begin{aligned} OC_{MG}(t) = \Delta t \cdot \{ & w_{\mathrm{b}} \cdot [P_{\mathrm{b}}^c(t) + P_{\mathrm{b}}^d(t)] + \\ & + \sum_{k=1}^{n_{EV}} [(w_{\mathrm{k}} + c_{ev}(t)) \cdot P_{ev,k}^c(t) + \\ & + (w_{\mathrm{k}} - r_{ev}(t)) \cdot P_{ev,k}^d(t)]\} \end{aligned} \qquad (3)$$

The optimization model is completed with the constraints related to the active power balance at dc busbar at each time-step t, as in (4)

$$\begin{aligned} & \eta_g \cdot P_g^{in}(t) - \frac{1}{\eta_g} \cdot P_g^{out}(t) + \eta_b \cdot P_b^d(t) - \frac{1}{\eta_b} \cdot P_b^c(t) + \\ & \sum_{k=1}^{n_{EV}} \left[\eta_{ev,k} \cdot P_{ev,k}^d(t) - \frac{1}{\eta_{ev,k}} \cdot P_{ev,k}^c(t) \right] + \eta_{PV} \cdot P_{PV}(t) = 0 \end{aligned} \qquad (4)$$

Coefficients η_x represent converter efficiencies and cable losses, according to [39]. Injected powers to the dc busbar are considered as positive, while withdrawn powers are negative. In (5) and (6) the evaluation of SOC for BES and EV batteries is evaluated at each time-step.

$$\begin{aligned} SOC_b(t) = SOC_b(t-1) + \Delta t \cdot \left[\gamma_b^c \cdot P_b^c(t) - \frac{1}{\gamma_b^d} \cdot P_b^d(t) \right] + \\ -sd_b \end{aligned} \qquad (5)$$

$$\begin{aligned} SOC_{ev,k}(t) = SOC_{ev,k}(t-1) + \Delta t \cdot [\gamma_{ev,k}^c \cdot P_{ev,k}^c(t) + \\ -\frac{1}{\gamma_{ev,k}^d} \cdot P_{ev,k}^d(t)] - sd_{ev,k} - \Delta E_{ev,k}^{trip}(t) \end{aligned} \qquad (6)$$

where $\Delta E_{ev,k}^{trip}(t)$ is different from zero only in traveling timesteps and estimated according to unit consumption depending on average speed.

In order to avoid contemporaneous bidirectional power exchange at grid connection, the following relations hold:

$$P_g^{in}(t) \leq \upsilon_g(t) \cdot P_{g,MAX}^{in} \qquad (7)$$

$$P_g^{out}(t) \leq (1 - \upsilon_g(t)) \cdot P_{g,MAX}^{out} \qquad (8)$$

where $\upsilon_g(t)$ takes value 1 if power is withdrawn and 0 if it is delivered. Analogous relations can be written for BES charge/discharge (limits $P_b^{c,nom}$ and $P_b^{d,nom}$ and variable $\upsilon_b(t)$)

and EVs (limits $P_{ev,k}^{c,nom}$ and $P_{ev,k}^{d,nom}$ and variable $\upsilon_{ev,k}(t)$) considering also SOC limits.

The two-stage procedure is illustrated in Fig. 1.

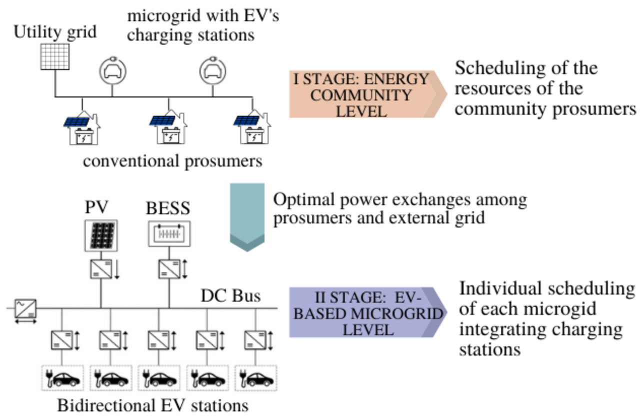

Fig. 1. Scheme of the two-stage optimal scheduling procedure.

B. *Stochastic approach for reserve provision by BES units*

The stochastic approach deals with the uncertainty related to the PV forecast, with the aim of guaranteeing the balance of generation and demand, and therefore the respect of the power exchange plan within the community calculated in the first stage, even in the presence of forecasting errors. The actual PV production $P_{PV}^{act}(t)$ is assumed to be dependent on the forecast value and a forecasting error:

$$P_{PV}^{act}(t) = P_{PV}(t) + \varepsilon_{PV}(t) \quad \forall t \in [1, n_t] \tag{9}$$

The net forecasting error $\varepsilon(t)$ is defined:

$$\varepsilon(t) = -\varepsilon_{PV}(t) \qquad \forall t \in [1, n_t] \tag{10}$$

A positive value of $\varepsilon(t)$ means that the system requires additional generation. On the contrary, negative values of the net forecasting error represent the case of the net requiring a decrease in generation. As $\varepsilon(t)$ could be positive or negative, it can be split into a positive and negative part:

$$\varepsilon(t) = \varepsilon^{+}(t) - \varepsilon^{-}(t) \qquad \forall t \in [1, n_t] \tag{11}$$

where $\varepsilon^{+}(t) = \max(\varepsilon(t), 0)$ and $\varepsilon^{-}(t) = \max(-\varepsilon(t), 0)$. This distinction is useful for the definition of the reserve to be provided by storage units.

A chance-constrained approach is adopted to define the level of positive and negative reserves - added to the vector of state variables - needed to compensate the forecasting error with high probability, in each time step:

$$Prob\left(\varepsilon^{+}(t) \le R_b^{+}(t)\right) \ge 1 - \alpha^{+}(t) \quad \forall t \in [1, n_t] \tag{12.a}$$

$$Prob\left(\varepsilon^{-}(t) \le R_b^{-}(t)\right) \ge 1 - \alpha^{-}(t) \quad \forall t \in [1, n_t] \tag{12.b}$$

Assuming that the network forecasting error is normally distributed, constraints (12) can be linearized and added in the second-stage problem such that positive and negative reserve levels should be at least equal to the $(1-\alpha^{+})$-th and $(1-\alpha^{-})$-th quantile of $\varepsilon(t)$ probability distribution:

$$\varepsilon(t) \to N\left(\mu_\varepsilon(t), \sigma_\varepsilon^2(t)\right) \tag{13}$$

$$R_b^{+}(t) \ge q_{1-\alpha^{+}}^{+}(t) \tag{14.a}$$

$$R_b^{-}(t) \ge q_{1-\alpha^{-}}^{-}(t) \tag{14.b}$$

Quantiles depend on the distribution parameters, as follows:

$$q_{1-\alpha^{+}}^{+}(t) = -\mu_\varepsilon(t) + N^{-1}\left(1-\alpha^{+}(t)\right) \cdot \sqrt{\sigma_\varepsilon^2(t)} \tag{15.a}$$

$$q_{1-\alpha^{-}}^{-}(t) = \mu_\varepsilon(t) - N^{-1}\left(\alpha^{-}(t)\right) \cdot \sqrt{\sigma_\varepsilon^2(t)} \tag{15.b}$$

The reserves that can be provided by each BES unit *b* at time *t* are limited by the actual available energy stored and the maximum charging/discharging powers:

$$R_b^{+}(t) \le \frac{SOC_b(t) - SOC_b^{\min}}{\Delta t} \tag{16}$$

$$R_b^{+}(t) \le P_b^{d,nom} - P_b^{d}(t) \tag{17}$$

$$R_b^{-}(t) \le \frac{SOC_b^{\max} - SOC_b(t)}{\Delta t} \tag{18}$$

$$R_b^{-}(t) \le P_b^{c,nom} - P_b^{c}(t) \tag{19}$$

C. *Inclusion of the reserve provision by a cluster of EV batteries*

The representation of the reserve provision of n_{ev} batteries of EVs connected to the charging stations requires the inclusion of positive and negative reserves, in the state vector. $R_{ev,k}^{+}(t)$ and $R_{ev,k}^{-}(t)$ are added in constraints (14.a) and (14.b):

$$\sum_{k=1}^{n_{ev}} R_{ev,k}^{+}(t) + R_b^{+}(t) \ge q_{1-\alpha^{+}}^{+}(t) \tag{20.a}$$

$$\sum_{k=1}^{n_{ev}} R_{ev,k}^{-}(t) + R_b^{-}(t) \ge q_{1-\alpha^{-}}^{-}(t) \tag{20.b}$$

For each EV *k* and time *t*, the constraints that limit EV power reserve considering actual SOC_{ev} levels and the rated values of the charging and discharging powers are:

$$R_{ev,k}^{+}(t) \le \frac{SOC_{ev,k}(t) - SOC_{ev,k}^{\min}}{\Delta t} \tag{21.a}$$

$$R_{ev,k}^{+}(t) \le P_{ev,k}^{d,nom} - P_{ev,k}^{d}(t) \tag{21.b}$$

$$R_{ev,k}^{-}(t) \le \frac{SOC_{ev,k}^{\max} - SOC_{ev,k}(t)}{\Delta t} \tag{22.a}$$

$$R_{ev,k}^{-}(t) \le P_{ev,k}^{c,nom} - P_{ev,k}^{c}(t) \tag{22.b}$$

IV. Case Study

The considered LEC involves five participants organized in one feeder and connected to the same low voltage network.

Three of them correspond to prosumers equipped with a PV unit, a BES unit and local loads. The rest of participants correspond to two microgrids, each equipped with a cluster of 5 EV bidirectional charging stations, a PV unit and a BES system. The optimization horizon corresponds to one day divided into 96 periods of 15 minutes. Fig. 2 shows the considered price profile of buying (π_{buy}^{t}) and selling (π_{sell}^{t}) energy from and to the external utility grid, respectively. Fig. 2 also shows the assumed profile of the PV power generation per installed panel area. For simplicity, the times when the EV are connected to the bidirectional charging stations is considered known. At the beginning and at the end of the day, all EV are connected to the charging stations with 90% of the battery capacity. Vehicles of microgrid 1 are disconnected due to travelling in the intervals 8:45-9:00, and 13:00-13:15, 17:15-17:30 for EV1, 10:00-10:30 and 13:30-14:30 for EV2, 10:30-10:45 and 12:45 am-13:30 for EV3, 9:00:15-10:15 for EV5, EV4 is always connected. Vehicles of microgrid 2 are disconnected due to single daily travel between 9:00-9:30 (EV1), 9:30-10:00 (EV3), 10:30-12:30 (EV4), 9:30-10:45 (EV5), EV2 is always connected. The energy reduction in the EV battery during each trip is, on average, equal to 1.5 kWh for each 15 min period.

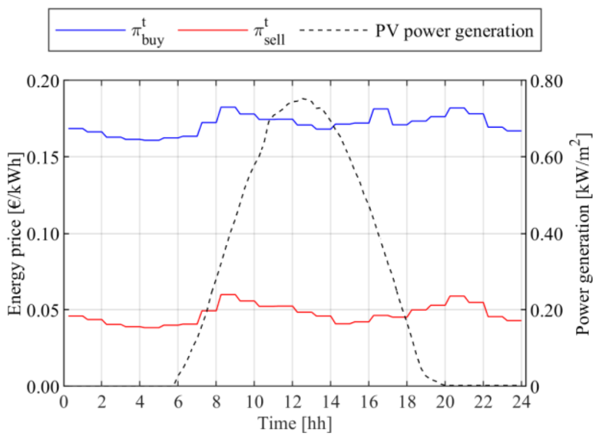

Fig. 2. Price profile of the grid (buying and selling) and profile PV power generation per m^2 of panel surface.

Other details on features of components for each LEC participant are reported in [34].

Positive and negative forecast errors of PV generation are modeled as Normal distributions. Mean μ_ε and standard deviation σ_ε values in each time-step are considered proportional to the forecast PV production, by means of δ_{PV} and ω_{PV} factors, respectively:

$$\mu_\varepsilon(t) = \delta_{PV} \cdot P_{PV}(t) \;\; \forall t \in [1, n_t] \tag{23.a}$$

$$\sigma_\varepsilon(t) = \omega_{PV} \cdot P_{PV}(t) \;\; \forall t \in [1, n_t] \tag{23.b}$$

where δ_{PV} is set at 0 and ω_{PV} is equal to 0.1. Constraint violation probabilities $\alpha^+(t)$ and $\alpha^-(t)$ are both set equal to 5% for each time-step. Fig. 3 shows the probability distribution functions of the error at specific times (namely, 9:00, 12:00 and 16:00) and the related positive quantile values. As expected, probability distribution at 12:00 is less steep than others at 9:00 and 16:00 characterized by lower σ_ε values. Similar observations hold for negative error probability distribution functions.

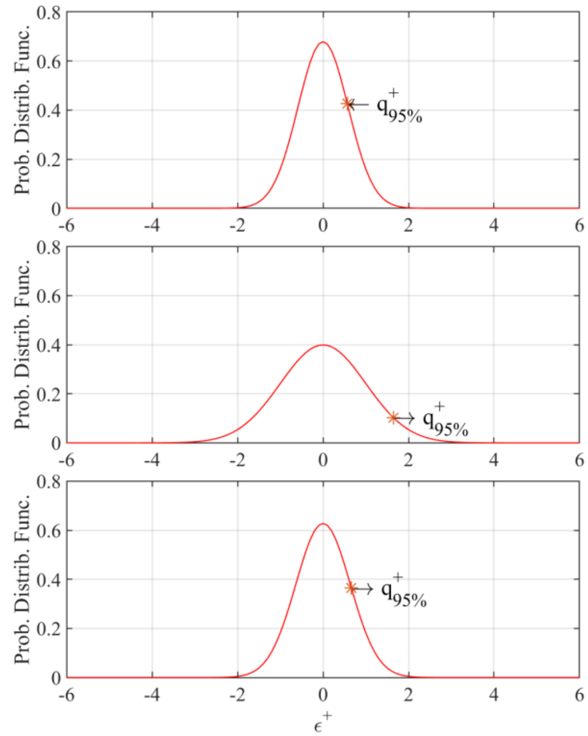

Fig. 3. Error probability distributions and positive quantile values relevant to the PV generation forecast at 9:00 (top), 12:00 (middle) and 16:00 (bottom).

V. Results

This section presents and discusses the final scheduling results, i.e., at the end of the second stage optimization. For both microgrids with clusters of EV charging stations involved in the community, the results obtained considering the reserve provision by BES units only are first presented in Section IV.A, then the results with reserve provision by both BES units and EV batteries are presented in Section IV.B.

A. Optimal BES units reserve provision

In Fig. 4 optimal power exchanges in microgrid 1 are shown, considering the reserve provided by the BES unit. Comparing to the results in [34] without reserve provision, all units in the microgrid follow a similar behavior. Reserve guaranteed with a probability of 90% by the BES unit (being $\alpha^+(t)$ and $\alpha^-(t)$ equal to 5%, as mentioned) is shown in Fig. 5. The maximum value of reserve (both positive and negative) to be provided is 1.7 kW at 12:30. The value of reserve increases considering lower values of $\alpha^+(t)$ and $\alpha^-(t)$. On the contrary, higher values of admitted violation probability implies lower values of reserve to be guaranteed. EV-based microgrid 2 power exchanges shown in Fig. 6 are slightly different from [34] in terms of EV exchange powers. Reserve provided is the same to microgrid 1 since the same error probability distribution is assumed.

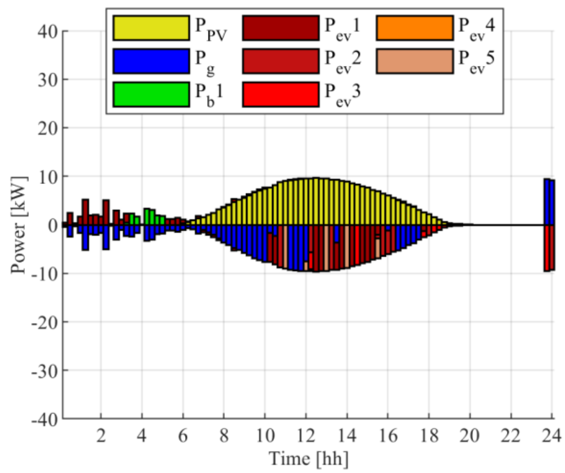

Fig. 4. Power exchanges in microgrid 1, considering the reserve provided by the BES unit.

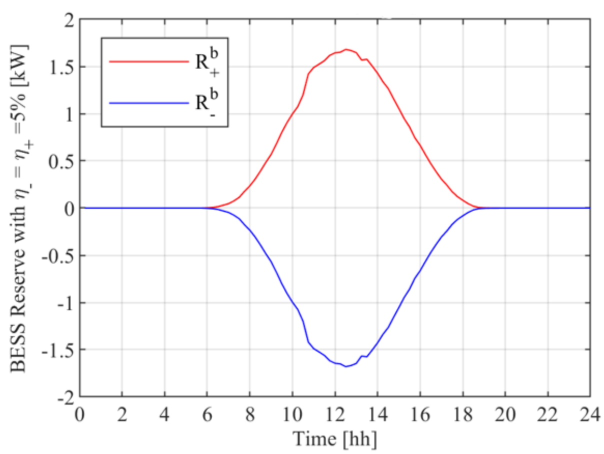

Fig. 5. Positive and negative reserve in microgrid 1 provided by the BES unit.

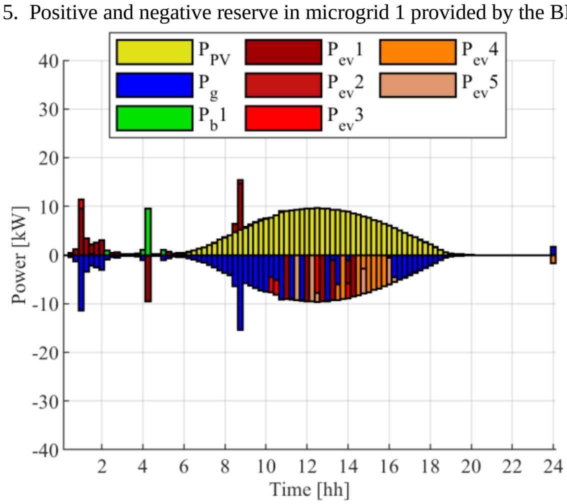

Fig. 6. Power exchanges in microgrid 2, considering the reserve provided by the BES unit.

B. Optimal BES and EV reserve provision

The inclusion of EV batteries in the reserve provision procedure affects the power exchanges within microgrids. In Fig. 7 the power exchanges in microgrid 1 are shown. From 00 to 06:00 BES discharging occurs to provide energy externally, then EVs and BES exchange energy among each other.

Fig. 8 shows the total positive and negative reserve dispatched among storage devices. Most reserve energy is provided by BES, since EV batteries cannot be available when EVs are not connected to the charging stations. Positive reserve corresponds to a discharging event, i.e., additional generation, while negative reserve represents a charging event of the storage, i.e., additional load.

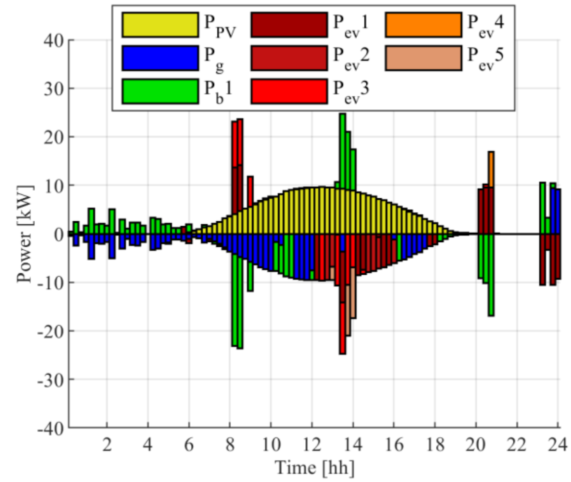

Fig. 7. Power exchanges in microgrid 1, considering the reserve provided by both the BES unit and the EV batteries.

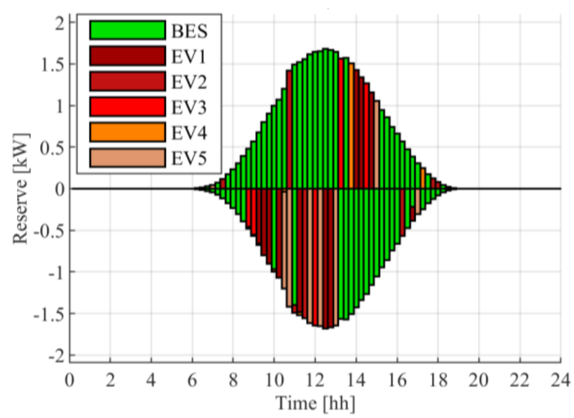

Fig. 8. Positive and negative reserve in microgrid 1 provided by both the BES unit and the EV batteries.

Fig. 9 compares the SOC level profiles of the BES unit and EV batteries of microgrid 1 for three cases: without reserve provision, when the reserve is provided only by the BES unit, and when the reserve is provided by both the BES unit and the EV batteries. No significant differences from the first case (no reserve provision operation) are shown in the profiles when the reserve is provided by the BES unit only. Different profiles are in general obtained, even for the SOC levels of the BES unit, when the reserve is provided also by the EVs connected to the charging stations. In the considered scenario, the BES unit experience significant discharges during the first hours of the day and between 13:00 and 14:00, EV1 discharges at 20:00, EV3 discharges at 08:00.

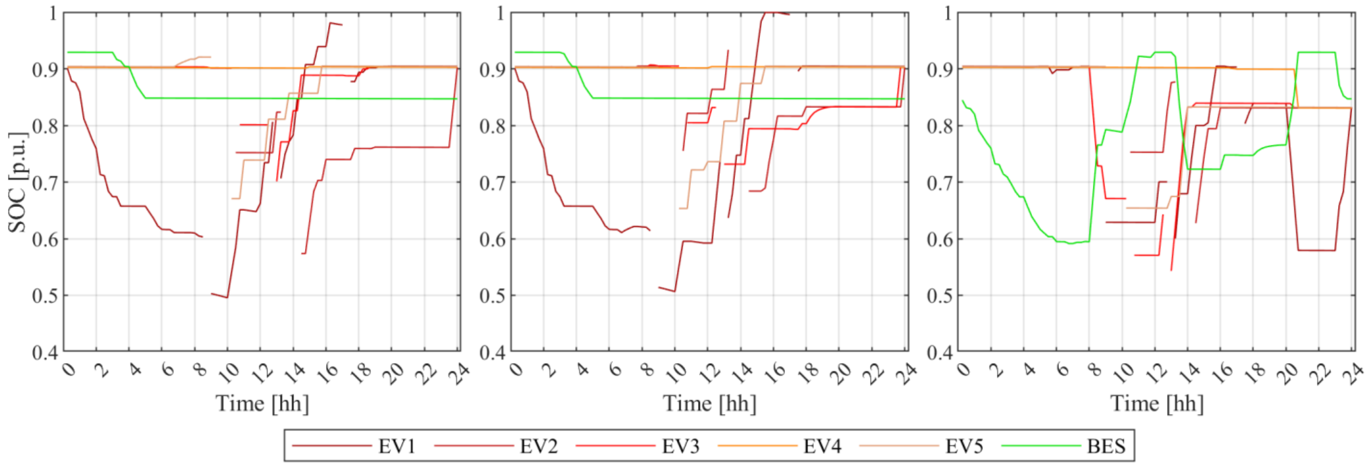

Fig. 9. SOC levels of BES unit and EV batteries in microgrid 1 considering no reserve provision (left), only reserve provided by BES (middle) and reserve provided by BES unit and EV batteries (right).

The different power exchanges in microgrid 2 are shown in Fig. 10, and the corresponding reserve provisions are shown in Fig. 11. Negative reserve is mostly provided by EV batteries. Like microgrid 1, the BES unit guarantees most of the positive reserve, especially in the first half of the daily PV production.

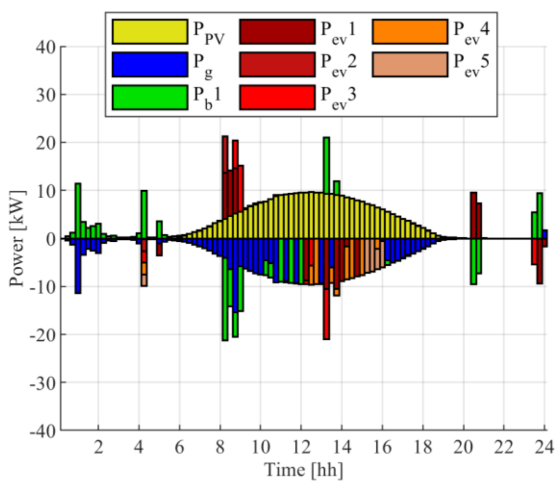

Fig. 10. Power exchanges in microgrid 2, considering the reserve provided by both the BES unit and the EV batteries.

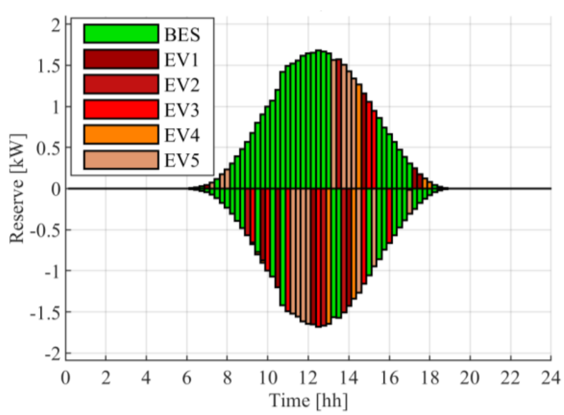

Fig. 11. Positive and negative reserve in microgrid 2 provided by both the BES unit and the EV batteries.

In Table I a comparison of the operating costs of each microgrid with EV charging stations in the two cases is carried out: when the reserve is provided only by the BES unit and when the reserve is provided by both the BES units and the EV batteries. The costs are evaluated considering the forecasted PV profile and the economic part OC_{MG}^{t} of objective function (3), without additional costs or revenues related to reserve provision. The daily costs of both EV-based microgrid are lower in the case the reserve is provided by both BES units and EV batteries. The benefit is expected to be lower when there is a significant uncertainty associated with the presence and state of charge of the EVs connected to the charging stations during the day. It should be remarked that for both the microgrids the daily operating cost of BES reserve case is very close to the values obtained in the deterministic procedure provided in [34].

TABLE I
DAILY OPERATING COSTS OF EV-BASED MICROGRIDS OF THE LEC

	BES reserve	BES and EV batteries reserve
microgrid 1	10.70 €	7.05 €
microgrid 2	7.92 €	5.17 €

C. *Validation of the chance constrained procedure*

In order to assess the advantages of the proposed chance constrained programming procedure, a comparison with the results of Monte-Carlo simulations is presented.

For microgrid 1, a set of 30 scenarios are considered, in which the PV production level at each timestep is varied by a stochastic quantity deriving from the error probability distribution functions defined in Section III.b, supposed independent from each other. The variations of PV production are depicted in Fig. 12. The results of the Monte-Carlo simulations are compared with the reserve levels, defined by (14.a) and (14.b) and illustrated in Fig. 5 and Fig. 8. Roughly 10% of samples lay beyond the reserve amount, in agreement with the considered $\alpha^{+}(t)$ and $\alpha^{-}(t)$ values.

Each scenario is analyzed by means of the deterministic technique described in [34], with the same objective function involving operation costs and variations from community-level power exchanges at grid connection point. In this way, for each scenario, different a scheduling of the microgrid devices (EVs, BESS, grid connection) is obtained, representing the effective exploitation of the chance-constrained reserve amounts in each particular situation.

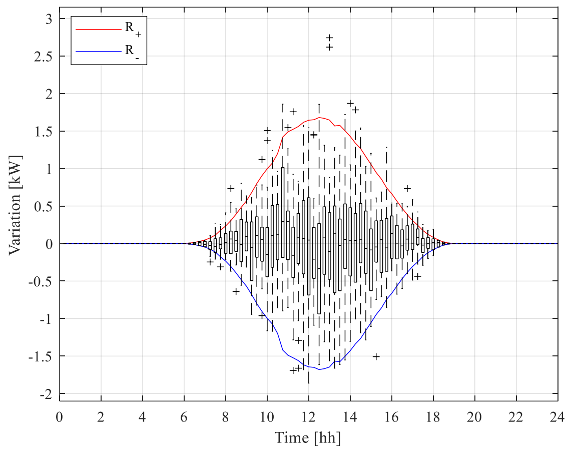

Fig. 12. Distribution of samples for PV production Monte-Carlo scenarios and comparison with reserve levels according to quantiles for microgrid 1.

The obtained results are summarized in Fig. 13 that shows the variation of grid exchanges and costs with respect to chance-constrained procedure outcomes. Monte-Carlo stochastic scenarios never reach solutions characterized by lower values of the objective function components than the corresponding ones in the chance-constrained formulation. In the majority of Monte-Carlo scenarios, grid power exchange levels are slightly varied – by less than 1.1 kWh at most – increasing the total bought energy.

The comparison with the Monte-Carlo simulation results shows that the chance-constrained procedure is able to find feasible and efficient solutions able to cope with PV forecasting error within the defined quantile levels.

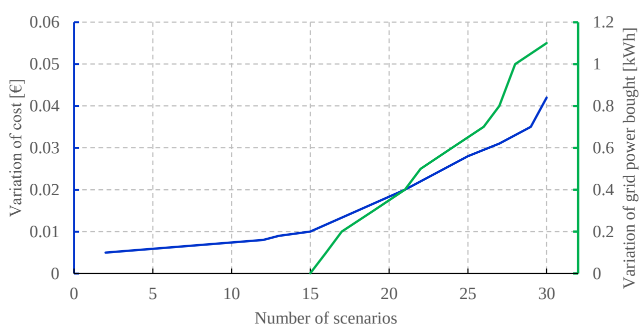

Fig. 13. Cumulative distribution of variation of grid energy bought in the Monte-Carlo scenarios (blue) and of daily operation costs (green) with respect to chance-constrained solution of microgrid 1.

VI. Conclusions

This paper focuses on the optimal planning of a local energy community involving dc microgrids with EV charging stations, considering the possibility for BES and EV batteries to provide a proper amount of reserve to counterbalance fluctuations in solar generation, modeled through a stochastic approach. In the framework of a two-stage scheduling procedure, in which the first stage defines the transaction among the community participants and with the external energy provider whilst the second stage defines the scheduling of each EV connected to the charging stations, a set of probabilistic chance constraints has been introduced in the second-stage optimization problem with the aim of modelling up and down reserves.

For a specific case study, calculations have been carried out considering reserve provision by BES units only or by both BES units and EV batteries. Positive and negative reserve amounts have been guaranteed during the day in both cases. However, the scheduling and the costs are different in the two cases. When the provision of reserve is only provided by the BES units there is no significant modification of the scheduled power exchanges within the microgrid with respect to the case when the reserve service is not considered. Whereas, when both BES units and EV batteries provides reserve, the scheduling differs and the daily costs of EV-based microgrids decrease, although neither specific revenues nor additional costs for reserve provision are considered.

The proposed chance-constrained approach enables the compliance with the community-level plan in the intraday operation and guarantees the achievement of low operational costs with reasonable computational effort.

The procedure could be improved by handling uncertainties concerning EV usage other than PV production. Moreover, the procedure will be integrated in the energy management system of a real installation.

References

[1] I. Campos, G. Pontes Luz, E. Marín-González, S. Gährs, S. Hall, L. Hostenkamp, “Regulatory challenges and opportunities for collective renewable energy prosumers in the EU,” *Energy Policy*, vol. 138, March 2020, n. 111212, doi: 10.1016/j.enpol.2019.111212

[2] Q. Li et *al.*, "Parallel and Distributed Optimization Method with Constraint Decomposition for Energy Management of Microgrids," *IEEE Transactions on Smart Grid*, vol. 12, no. 6, pp. 4627-4640, Nov. 2021, doi: 10.1109/TSG.2021.3097047.

[3] B. Zhou *et al.*, "Multi-microgrid Energy Management Systems: Architecture, Communication, and Scheduling Strategies," *Journal of Modern Power Systems and Clean Energy*, vol. 9, no. 3, pp. 463-476, May 2021, doi: 10.35833/MPCE.2019.000237.

[4] J. L. Martínez-Ramos *et al.*, "Provision of Ancillary Services by a Smart Microgrid: An OPF Approach," *2018 International Conference on Smart Energy Systems and Technologies* (SEST), 2018, pp. 1-6, doi: 10.1109/SEST.2018.8495883.

[5] M. Alowaifeer, *et al.*, "Grid Services Optimization from Multiple Microgrids," *IEEE Transactions on Smart Grid*, vol. 13, no. 1, pp. 8-19, Jan. 2022, doi: 10.1109/TSG.2021.3101235.

[6] M. Mao, Y. Wang, L. Chang and Y. Du, "Operation optimization for multi-microgrids based on centralized-decentralized hybrid hierarchical energy management," *2017 IEEE Energy Conversion Congress and Exposition*, 2017, pp. 4813-4820, doi: 10.1109/ECCE.2017.8096818.

[7] W. Zhang and Y. Xu, "Distributed optimal control for multiple microgrids in a distribution network," in *IEEE Transactions on Smart Grid*, vol. 10, no. 4, pp. 3765-3779, July 2019, doi: 10.1109/TSG.2018.2834921.

[8] A. Sinha, P. Malo and K. Deb, "A Review on Bilevel Optimization: From Classical to Evolutionary Approaches and Applications," in *IEEE Transactions on Evolutionary Computation*, vol. 22, no. 2, pp. 276-295, April 2018, doi: 10.1109/TEVC.2017.2712906.

[9] E. Fernandez *et al.*, "A Bi-level optimization-based community energy management system for optimal energy sharing and trading among peers." *Journal of Cleaner Production*, vol. 279, January 2021, doi: 10.1016/j.jclepro.2020.123254

[10] S. Bahramara, M. Parsa Moghaddam, and M. R. Haghifam. "A bi-level optimization model for operation of distribution networks with micro-grids." *International Journal of Electrical Power & Energy Systems*, vol. 82, pp. 169-178, November 2016, doi: 10.1016/j.ijepes.2016.03.015.

[11] C. Guo, X. Wang, Y. Zheng, F. Zhang, "Optimal energy management of multi-microgrids connected to distribution system based on deep reinforcement learning" *International Journal of Electrical Power & Energy Systems*, vol. 131, Oct. 2021, doi: 10.1016/j.ijepes.2021.107048.

[12] D. Wang, F. Locment, M. Sechilariu. "Modelling, simulation, and management strategy of an electric vehicle charging station based on a DC microgrid." *Applied Sciences*, vol. 10, issue 6, March 2020, 2053, doi: 10.3390/app10062053.

[13] J. Zhang *et al*., "A hierarchical distributed energy management for multiple PV-based EV charging stations" *IECON 2018-44th Annual Conference*. IEEE, 2018, doi: 10.1109/IECON.2018.8591742

[14] M.J. Shin, D.H. Choi, J. Kim. "Cooperative management for PV/ESS-enabled electric vehicle charging stations: a multiagent deep reinforcement learning approach." *IEEE Transactions on Industrial Informatics*, vol. 16, no. 5, pp. 3493-3503, May 2020, doi: 10.1109/TII.2019.2944183.

[15] M. Dicorato, G. Tricarico, F. Marasciuolo, G. Forte and M. Trovato, "Performance analysis of EV stations optimal operation in DC microgrid configurations," *2020 EEEIC / I&CPS Europe*, 2020, pp. 1-6, doi: 10.1109/EEEIC/ICPSEurope49358.2020.9160758

[16] H. Kikusato *et al*., “Electric Vehicle Charge-Discharge Management for Utilization of Photovoltaic by Coordination between Home and Grid Energy Management Systems,” *IEEE Trans. Smart Grid*, vol. 10, no. 3, pp. 3186–3197, 2019, doi: 10.1109/TSG.2018.2820026.

[17] A. Borghetti, F. Napolitano, S. Rahmani-Dabbagh, and F. Tossani, “Scenario tree generation for the optimization model of a parking lot for electric vehicles,” in *2017 AEIT International Annual Conference*, 2017, doi: 10.23919/AEIT.2017.8240519.

[18] M. Dicorato, G. Forte, M. Trovato, C. Boigues Muñoz, G. Coppola, “An integrated DC microgrid solution for electric vehicle fleet management”, *IEEE Trans. Ind. Appl.*, vol. 55, no. 6, Nov-Dec. 2019, pp. 7374-7355, doi: 10.1109/TIA.2019.2926359.

[19] S. Bruno, C. Iurlaro, M. La Scala, M. Menga, "Integration of Operating Reserve Constrains in the Predictive Optimal Dispatch of Energy and Storage Resources in Small Islands," EEEIC / I&CPS Europe, 2022, pp. 1-6, doi: 10.1109/EEEIC/ICPSEurope54979.2022.9854789.

[20] F. Marasciuolo *et al.*, "The Influence of EV Usage Scenarios on DC Microgrid Techno-Economic Operation," in *IEEE Transactions on Industry Applications*, vol. 58, no. 3, pp. 3957-3966, May-June 2022, doi: 10.1109/TIA.2022.3159298.

[21] S. S. Reddy, V. Sandeep, C.M. Jung, "Review of stochastic optimization methods for smart grid", *Front. Energy*, vol. 11, issue 2, Mar. 2017, pp. 197–209, doi: 10.1007/s11708-017-0457-7.

[22] G. Mohy-ud-din, K. M. Muttaqi, D. Sutanto, "A Cooperative Energy Transaction Model for VPP Integrated Renewable Energy Hubs in Deregulated Electricity Markets," in IEEE Transactions on Industry Applications, vol. 58, no. 6, pp. 7776-7791, Nov.-Dec. 2022, doi: 10.1109/TIA.2022.3195965.

[23] X. Deng, Q. Zhang, Y. Li, T. Sun and H. Yue, "Hierarchical Distributed Frequency Regulation Strategy of Electric Vehicle Cluster Considering Demand Charging Load Optimization," 2020 IEEE 3rd Student Conference on Electrical Machines and Systems (SCEMS), 2020, pp. 959-969, doi: 10.1109/SCEMS48876.2020.9352296.

[24] Y. Li, *et al.*, "Optimal Scheduling of Integrated Demand Response-Enabled Community-Integrated Energy Systems in Uncertain Environments," *IEEE Trans. on Industry Applications*, vol. 58, no. 2, pp. 2640-2651, March-April 2022, doi: 10.1109/TIA.2021.3106573.

[25] J. Liu, H. Chen, W. Zhang, B. Yurkovich, G. Rizzoni, "Energy management problems under uncertainties for grid-connected microgrids: a chance constrained programming approach," in *IEEE Transactions on Smart Grid*, vol. 8, no. 6, pp. 2585-2596, Nov. 2017, doi: 10.1109/TSG.2016.2531004.

[26] C. Orozco *et al.*, "Intra-day scheduling of a local energy community coordinated with day-ahead multistage decisions" *Sust. Energy, Grids and Networks*, vol. 29, March 2022, doi: 10.1016/j.segan.2021.100573.

[27] S. Bahramara *et al.*, "Modeling the Microgrid Operator Participation in Day-Ahead Energy and Reserve Markets Considering Stochastic Decisions in the Real-Time Market," IEEE Transactions on Industry Applications, vol. 58, no. 5, pp. 5747-5762, Sept.-Oct. 2022, doi: 10.1109/TIA.2022.3178386.

[28] Y. Cui, Z. Hu, H. Luo, "Optimal Day-Ahead Charging and Frequency Reserve Scheduling of Electric Vehicles Considering the Regulation Signal Uncertainty," IEEE Transactions on Industry Applications, vol. 56, no. 5, pp. 5824-5835, Sept.-Oct. 2020, doi: 10.1109/TIA.2020.2976839.

[29] N. Rezaei, A. Khazali, M. Mazidi, A. Ahmadi, "Economic energy and reserve management of renewable-based microgrids in the presence of electric vehicle aggregators: A robust optimization approach", *Energy*, vol. 201, June 2020, doi: 10.1016/j.energy.2020.117629.

[30] S. Bahramara, P. Sheikhahmadi, A. Mazza, G. Chicco, "Day-ahead self-scheduling from risk-averse microgrid operators to provide reserves and flexible ramping ancillary services." *International Journal of Electrical Power & Energy Systems*, vol. 142 Part B, November 2022, doi: 10.1016/j.ijepes.2022.108381.

[31] X. Yan et al., "An IGDT-Based Day-Ahead Co-Optimization of Energy and Reserve in a VPP Considering Multiple Uncertainties," in *IEEE Transactions on Industry Application*s, vol. 58, no. 3, pp. 4037-4049, May-June 2022, doi: 10.1109/TIA.2022.3152454.

[32] Z. Liu, L. Wang, L. Ma, "A transactive energy framework for coordinated energy management of networked microgrids with distributionally robust optimization," *IEEE Trans. on Power Systems*, vol. 35, no. 1, pp. 395-404, Jan. 2020, doi: 10.1109/TPWRS.2019.2933180.

[33] W. Huang, W. Zheng and D. J. Hill, "Distributionally Robust Optimal Power Flow in Multi-Microgrids with Decomposition and Guaranteed Convergence," in IEEE Transactions on Smart Grid, vol. 12, no. 1, pp. 43-55, Jan. 2021, doi: 10.1109/TSG.2020.3012025.

[34] F. Marasciuolo, C. Orozco, M. Dicorato, A. Borghetti, G. Forte, "Two-stage Scheduling of Electrical Vehicle Charging Station Clusters in a Community of DC Microgrids," *EEEIC / I&CPS Europe, 2021*, pp. 1-6, doi: 10.1109/EEEIC/ICPSEurope51590.2021.9584584.

[35] T. Zhao *et al.*, "Real-Time Optimal Energy and Reserve Management of Electric Vehicle Fast Charging Station: Hierarchical Game Approach," in *IEEE Trans. on Smart Grid*, vol. 9, no. 5, pp. 5357-5370, Sept. 2018, doi: 10.1109/TSG.2017.2687522.

[36] I. Pavić, H. Pandžić and T. Capuder, "Electric Vehicle Aggregator as an Automatic Reserves Provider Under Uncertain Balancing Energy Procurement," in IEEE Transactions on Power Systems, vol. 38, no. 1, pp. 396-410, Jan. 2023, doi: 10.1109/TPWRS.2022.3160195.

[37] M. Dicorato, M. Trovato, G. Forte, “Operation schedule of DC microgrid for EVs with reserve under various conditions”, Proc of 2019 AEIT, pp. 1-5, Sept. 2019, doi: 10.23919/AEIT.2019.8893412 .

[38] S. Lilla, C. Orozco, A. Borghetti, F. Napolitano, and F. Tossani, “Day-ahead scheduling of a local energy community: an alternating direction method of multipliers approach,” *IEEE Trans. Power Syst.*, vol. 35, no. 2, pp. 1132–1142, 2020, doi: 10.1109/TPWRS.2019.2944541.

[39] B. Aluisio, *et al.*, “DC-Microgrid Operation Planning for an electric vehicle supply infrastructure,” *Applied Sciences*, vol. 9, no, 13, Jul-1 2019, 2687, doi: 10.3390/app9132687.